Neuroprotective Effects of Protein Tyrosine Phosphatase 1B Inhibition against ER Stress-Induced Toxicity

Yu-Mi Jeon[1], Shinrye Lee[1], Seyeon Kim[1], Younghwi Kwon[1], Kiyoung Kim[2], Chang Geon Chung[3], Seongsoo Lee[4], Sung Bae Lee[3], and Hyung-Jun Kim[1,*]

[1]Department of Neural Development and Disease, Korea Brain Research Institute (KBRI), Daegu 41068, Korea, [2]Department of Medical Biotechnology, Soonchunhyang University, Asan 31538, Korea, [3]Department of Brain & Cognitive Sciences, Daegu Gyeongbuk Institute of Science and Technology (DGIST), Daegu 42988, Korea, [4]Gwangju Center, Korea Basic Science Institute (KBSI), Gwangju 61186, Korea
*Correspondence: kijang1@kbri.re.kr
http://dx.doi.org/10.14348/molcells.2017.2320
www.molcells.org

Several lines of evidence suggest that endoplasmic reticulum (ER) stress plays a critical role in the pathogenesis of many neurodegenerative diseases such as Alzheimer's disease, Parkinson's disease, and amyotrophic lateral sclerosis. Protein tyrosine phosphatase 1B (PTP1B) is known to regulate the ER stress signaling pathway, but its role in neuronal systems in terms of ER stress remains largely unknown. Here, we showed that rotenone-induced toxicity in human neuroblastoma cell lines and mouse primary cortical neurons was ameliorated by PTP1B inhibition. Moreover, the increase in the level of ER stress markers (eIF2α phosphorylation and PERK phosphorylation) induced by rotenone treatment was obviously suppressed by concomitant PTP1B inhibition. However, the rotenone-induced production of reactive oxygen species (ROS) was not affected by PTP1B inhibition, suggesting that the neuroprotective effect of the PTP1B inhibitor is not associated with ROS production. Moreover, we found that MG132-induced toxicity involving proteasome inhibition was also ameliorated by PTP1B inhibition in a human neuroblastoma cell line and mouse primary cortical neurons. Consistently, downregulation of the PTP1B homologue gene in *Drosophila* mitigated rotenone- and MG132-induced toxicity. Taken together, these findings indicate that PTP1B inhibition may represent a novel therapeutic approach for ER stress-mediated neurodegenerative diseases.

Keywords: endoplasmic reticulum stress (ER Stress), MG132, reactive oxygen species (ROS), rotenone, ubiquitin proteasome system

INTRODUCTION

The endoplasmic reticulum (ER) is a multifunctional continuous membrane system essential for the synthesis, folding and processing of secretory and transmembrane proteins in eukaryotic cells. Functional impairment of the ER causes accumulation of unfolded proteins in the ER lumen and leads to an evolutionarily conserved stress response called the unfolded protein response (Chung et al., 2015; Xu et al., 2005). Previous studies have indicated that prolonged ER stress is implicated in many human diseases including neurodegenerative diseases, atherosclerosis, type 2 diabetes and cancer (Ozcan and Tabas, 2012).

Protein tyrosine phosphatase 1B (PTP1B) is a ubiquitously expressed enzyme anchored in the ER membrane (Popov, 2012). PTP1B plays a crucial role in ER homeostasis through dephosphorylating tyrosine kinase receptors and thereby

regulating the intensity of their signaling cascades (Popov, 2012). Previous studies have indicated that ER stress elevated by a high-fat diet is attenuated by PTP1B deletion in mouse skeletal muscle (Panzhinskiy et al., 2013a). In the central nervous system, neuron-specific PTP1B deletion mice are hypersensitive to leptin and have reduced body weight (Prada et al., 2013). Moreover, PTP1B upregulation is observed in neuroinflammatory conditions. Rat spinal cord injury greatly increases the level of PTP1B in motor neurons, and brain injection of lipopolysaccharide (LPS, inflammation inducer) significantly elevates PTP1B expression (Song et al., 2016; Zhu et al., 2015). Collectively, this evidence suggests that PTP1B seems to play an important role in ER stress-mediated neuronal cell death, though the mechanism underlying its role in neuronal ER stress is mostly unknown.

To investigate the role of PTP1B in ER stress-mediated neuronal cell death, we treated the neuroblastoma cell line (SH-SY5Y) and mouse primary cortical neurons with ER stress inducers such as rotenone and MG132. Rotenone produces reactive oxygen species (ROS) through mitochondrial complex I inhibition (Nandipati and Litvan, 2016), and MG132 is a specific inhibitor of the 26S proteasome (Cui et al., 2013). Even though the two chemicals induce ER stress via different mechanisms, PTP1B inhibition mitigated both MG132 and rotenone-induced neuronal cell death. Furthermore, PTP1B inhibition decreased the level of ER stress markers such as phosphorylated eIF2 alpha and phosphorylated PERK. In addition, downregulation of the *PTP1B* homologue gene in *Drosophila* mitigated rotenone and MG132 toxicity. Taken together, our findings indicate that PTP1B inhibition may represent a novel therapeutic approach for ER stress mediated neurodegenerative diseases.

MATERIALS AND METHODS

Reagents and antibodies
Cell culture media and fetal bovine serum (FBS) were obtained from Thermo Fisher Scientific (USA). Rotenone (R8875), dimethyl sulfoxide, 2′,7′-dichlorofluorescein diacetate and tunicamycin (T7765) were purchased from Sigma-Aldrich (USA). The PTP1B (CAS-765317-72-4) inhibitor and MG132 were purchased from EMD Millipore (USA). Rabbit anti-phospho-eIF2a (Ser51) (catalog no. 3597), rabbit anti-eIF2a (catalog no. 9722) and HRP-conjugated anti-alpha-tubulin (catalog no. 9099) were obtained from Cell Signaling Technology. Rabbit anti-phospho-PERK (Thr981) (catalog no. sc32577) and rabbit anti-PTP1B (catalog no. sc14021) were purchased from Santa Cruz Biotechnology.

Cell culture and cell viability assay
Human neuroblastoma cells, SH-SY5Y, were grown in DMEM with 10% fetal bovine serum (FBS) and anti-biotic (100 U/ml penicillin, 100 μg/ml streptomycin) solutions at 37℃ in 5% CO_2/95% air. SH-SY5Y cells were seeded in 96-well plates (1×10^5 cells/well). After 24 h, different treatments were performed. Cortical tissue from embryonic day 16 (E16) mouse brains was dissected out, incubated with 0.25% trypsin for 15 min at 37℃, and dissociated by mechanical trituration (Araki et al., 2000). The brains was re-

moved and transferred to a 15 ml conical tube and washed twice with ice-cold HBSS (Gibco), and the cortex was separated and then incubated with 2 ml of pre-warmed papain (20 units/ml) (Worthington Biochemical Corporation) and DNase I (0.005%) for 30 min at 37℃ in a humidified cell culture incubator supplied with 5% CO_2. After incubation, cortical cells were centrifuged at 800 rpm for 10 min at room temperature. Dissociated cortical neurons were then plated in 48-well plates (2×10^5 cells/well) previously coated with 0.1% poly-D-lysine (Sigma-Aldrich), and grown in neurobasal media containing B27 supplement (Gibco), N2 supplement (Gibco), 2 mM glutamine (Gibco), and penicillin-streptomycin (Gibco). The culture media was changed initially after 5 days and then half-changed every 3 days, and cells were used after culture for 14-15 days.

Finally, the viability of the cells was determined by using the Cell Counting Kit-8 (CCK-8) assay, as previously described (Xu et al., 2012). CCK-8 is more sensitive than the 3-(4,5-dimethylthiazol-2-yl)-2,5-diphenyltetrazolium bromide assay. For dose-response studies of rotenone toxicity, SH-SY5Y cells and primary cortical neurons were cultured with rotenone at 0-1000 μM and 0-20 μM concentrations for 24 h, respectively. Then, for dose-response studies of MG132 toxicity, SH-SY5Y cells and primary cortical neurons were cultured with MG132 at 0-20 μM and 0-1 μM concentrations for 24 h, respectively. Finally, for dose-response studies of tunicamycin toxicity, SH-SY5Y cells were cultured with tunicamycin at 0-20 μM concentrations for 24 h. Then, 10-20 μl CCK-8 (Enzo Life Sciences) solution was added to each well. Plates were incubated for an additional 2 h. The optical density of each well was measured using a microplate reader (Tecan) at a 450 nm wavelength. Cell viability was expressed as a percentage of that of the DMSO-treated cells. All experiments were performed in triplicate.

Fly strains
Drosophila stocks were raised at 24℃ on standard cornmeal agar media with a 12 h dark-light cycle. The following *Drosophila* strains were obtained from the Bloomington *Drosophila* Stock Center (USA, http://flystocks.bio-indiana.edu/): w^{1118} as wild type; Da-Gal4 that drives ubiquitous transgene expression and UAS-*Ptp61f* RNAi (RNAi knockdown of *Ptp61f*).

Fly survival assay
Flies (n < 100) from each experimental group were monitored for their survival along with aging. The rotenone, paraquat and MG132-induced toxicity survival assays were performed on regular food medium. Flies were maintained on standard cornmeal agar media at 24℃ and transferred every day to a new vial containing food that was treated with chemicals for the chemical treatment groups. Next, a survival assay was performed on filter papers soaked with 450 μM MG132 and 5% sucrose at 30℃. Filters were changed daily. The non-chemical treatment groups were maintained in the same way except for the treatment with the chemicals. The percentage of flies that remained alive at the end of the experiment was calculated based on the starting number of flies for each treatment group. This experiment was repeat-

ed three times.

Intracellular ROS assay

The levels of intracellular ROS generation were evaluated by DCFH-DA as previously described (Song et al., 2012). Briefly, after treatment, cells were washed with 1X PBS and loaded with DCFH-DA (final concentration 10 μM in colorless DMEM) for 30 min at 30℃. Fluorescence was measured by using a fluorescence spectrophotometer with excitation at 485 nm and emission at 530 nm.

Measurement of oxygen consumption rate (OCR)

The OCR was measured using a Seahorse XF24 analyzer according to the manufacturer's instructions (Seahorse Bio-science Inc). Briefly, SH-SY5Y cells were plated at 1×10^5 cells per well in full growth medium (Hardie et al., 2017). After overnight attachment, the medium was washed and replaced with pre-warmed running medium (non-buffered DMEM supplemented with 4 mM L-glutamine, 25 mM D-glucose and 1 mM sodium pyruvate, pH 7.4) and incubated in a non-CO_2 incubator at 37℃ for 60 min. The OCR was further measured following injection of rotenone and the PTP1B inhibitor. After the OCR measurement, cells were lysed, and the protein content was estimated using a BCA Assay (Pierce). The OCR was plotted after normalizing by total protein.

Immunoblotting assay

After treatment, the cells were homogenized in RIPA buffer (Cell signaling Technology) with a phosphatase and protease inhibitor cocktail (Roche) and incubated at 4℃ for 1 h. Cells were collected by centrifugation at 13,000 rpm for 30 min at 4℃. The supernatant was collected, and the protein concentration was determined using a BCA protein assay kit (Pierce). Next, denatured proteins were separated by Nu-PAGE 4-12% Bis-Tris Gels (Novex) and transferred to a polyvinylidene difluoride (PVDF) membrane (Novex) at 20 V for 1 h. The blots were blocked for 1 h at room temperature in 5% skim milk. The membrane was then incubated overnight at 4℃ with primary antibodies against phospho-eIF2a (Ser51), eIF2a, phospho-PERK (Thr981), PTP1B and α-tubulin. The membrane was incubated for 1 h with HRP-conjugated secondary antibodies, followed by detection with the ECL prime kit (Amersham Biosciences). Samples from three independent experiments were used in this analysis. The relative expression level was determined by using a Fusion-FX imaging system (Viber Lourmat).

Flow cytometry analysis

Cell death was detected by using an FITC Annexin V apoptosis detection kit (BD Biosciences) and flow cytometry. In brief, cells were trypsinized and washed with chilled PBS twice, and the cell pellets were re-suspended in binding buffer (10 mM HEPES, 140 mM NaCl, 2.5 mM CaCl2, pH 7.4) to create a cell suspension at a density of 1×10^6 cells/ml. Then, 3 μl of FITC-conjugated Annexin V was added to the suspension, which was incubated for 15 min at room temperature in the dark. Finally, 3 μl of propidium iodide was added, and flow cytometry was performed within 1 h using MoFlo Astrios cell

sorter (Beckman Coulter).

Statistical analyses

Each experiment was performed at least three times, and the results were presented as the means ± standard deviations (SD) or means ± standard error (SEM). Comparison between groups was made by one-way analysis of variance (ANOVA) followed by Tukey's multiple comparisons test (GraphPad Prism Software) or analyzed by Student's *t*-test. A value of $p < 0.05$ was deemed to be statistically significant and is indicated as follows: *$p < 0.05$; **$p < 0.005$; n.s., not significant.

RESULTS

PTP1B inhibition protects mammalian neuronal cells against rotenone-induced cell death

To investigate the role of PTP1B in neuronal ER stress, we used rotenone-treated SH-SY5Y cells and a selective PTP1B inhibitor (CAS 765317-72-4) (Wiesmann et al., 2004). Rotenone is a widely used insecticide and is known to induce ER stress via ROS production (Pal et al., 2014). The cytotoxicity of the human neuroblastoma cell line (SH-SY5Y) was determined using a CCK-8 assay, and the percent cell viability was plotted. Treatment with rotenone (15 μM for 24 h) reduced cell viability by approximately 50% in SH-SY5Y cells (Fig. 1A). Pre-treatment with the PTP1B inhibitor at concentrations ranging from 5-20 μM reduced rotenone-induced cell death in a dose-dependent manner (Fig. 1A). Furthermore, PTP1B inhibition mitigated rotenone-induced toxicity in primary mouse cortical neurons (Fig. 1B, 53% compared to 68% in rotenone-treated primary cortical neuronal cells). The protective effect of the PTP1B inhibitor on rotenone-induced toxicity was also assessed by PI and Annexin V staining followed by flow cytometric analysis in SH-SY5Y cells. Annexin V and PI were used to determine the levels of apoptotic cell death (PI^-/Annexin V^+ or PI^+/Annexin V^+) or necrotic cell death (PI^+/Annexin V^-). Rotenone induced cell death in 25.79% of SH-SY5Y cells (PI^-/Annexin V^+ or PI^+/Annexin V^+: 20.94% and PI^+/Annexin V^-: 4.85%). In comparison, the percent cell death in SH-SY5Y cells treated with both rotenone and the PTP1B inhibitor was 8.84% (PI^-/Annexin V^+ or PI^+/Annexin V^+: 6.77% and PI^+/Annexin V^-: 2.07%). PTP1B inhibitor pretreatment decreased cell death by 16.95% in the rotenone-treated condition, whereas the PTP1B inhibitor alone without rotenone treatment did not affect neuronal viability (Fig. 1C). These data indicate that PTP1B inhibition protects neuronal cells from rotenone-induced cell death.

PTP61F inhibition antagonizes oxidative stress-induced toxicity in *Drosophila*

We next investigated the role of PTP1B in ROS-induced toxicity *in vivo* using *Drosophila*. We knocked down *Ptp61f*, the *Drosophila* homologue of PTP1B, by RNAi in the presence of ROS inducers (paraquat or rotenone) and examined the effect of PTP1B knockdown on the ROS-induced death of flies. Paraquat is a highly toxic herbicide that produces oxidative stress through generation of superoxide anion (Day et al., 1999). *Ptp61f* downregulation in the whole body was
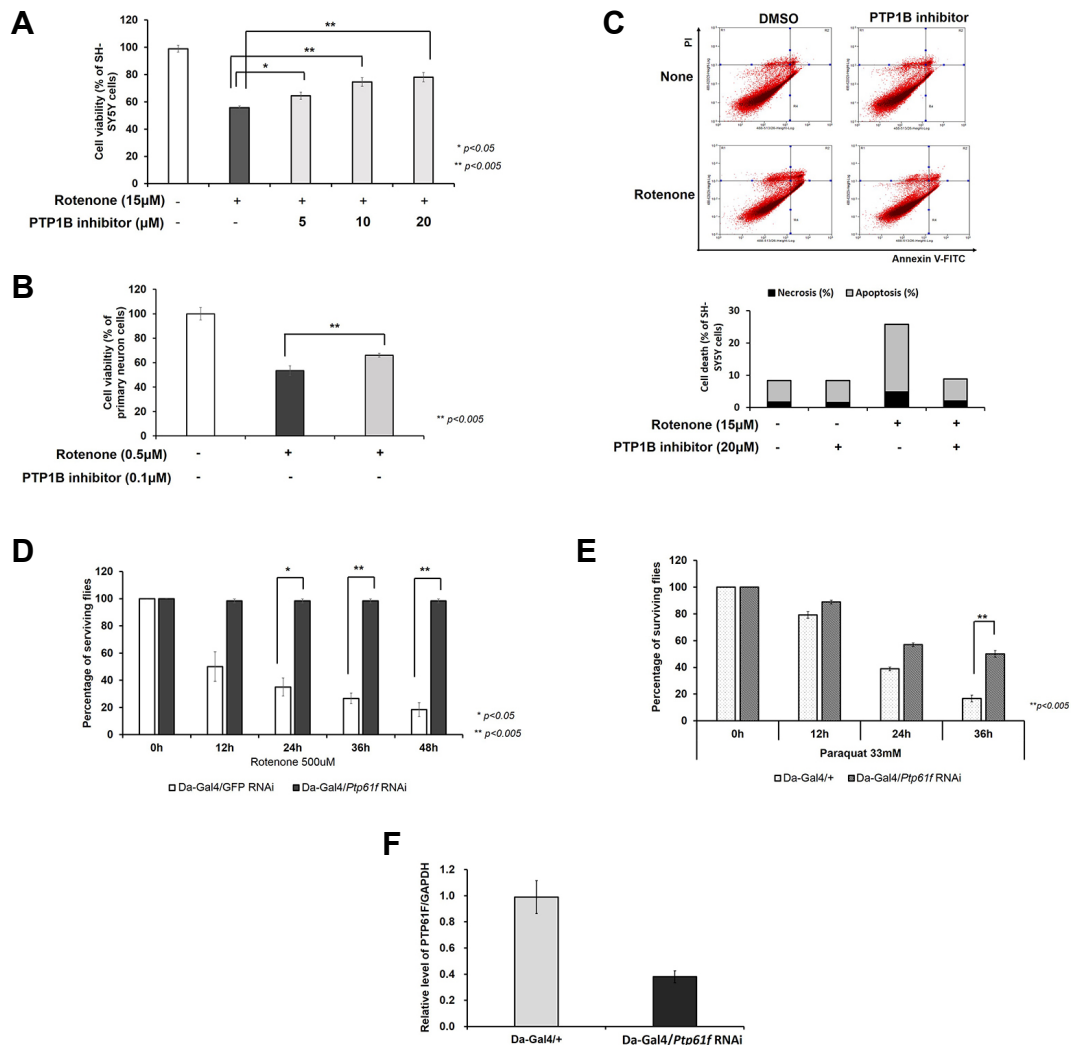
Fig. 1. ROS-induced toxicity is mitigated by PTP1B inhibition. SH-SY5Y cells (A) and primary mouse cortical neuron (B) cells were pretreated with various concentrations of the PTP1B inhibitor for 30 min and then treated with rotenone for 24 h. The rotenone-induced increase in neuronal cell death was attenuated by PTP1B inhibition. The cell viability was then determined by CCK-8 assay, and the percentage of cell viability was plotted as the mean ± SD of the three different experiments (*$p < 0.05$, **$p < 0.005$, One-way ANOVA with Tukey's multiple comparison test). (C) SH-SY5Y cells were pretreated with or without the PTP1B inhibitor (20 μM) and DMSO only for 30 min and then were exposed to rotenone for 24 h. Cell death was measured using the Annexin V/PI double staining assay analyzed by flow cytometry. PTP1B inhibition mitigated the rotenone-induced toxicity compared with that in the control cells. Quantification of the percentage of cell death was based on the flow cytometric analysis (lower). *Ptp61f* (*Drosophila* homolog of mammalian PTP1B) RNAi in whole tissue (Da-Gal4) improves survival rates following exposure to 500 μM rotenone (D) and 33 mM paraquat (E). Quantification of the percentage of surviving flies. The rotenone- or paraquat-reduced lifespan was significantly extended by downregulation of *Ptp61f* in the whole body. (F) Real time-PCR for *Ptp61f* mRNA levels. RNAi-mediated knockdown of *Ptp61f* in *Drosophila* reduced the expression of *Ptp61f* mRNA transcript levels. Quantification of mRNA transcript levels from 3-5 independent experiments, normalized to GAPDH. Genotypes: Control is *Da-Gal4/GFP RNAi*, *Da-Gal4/+* and *Ptp61f* RNAi is *Da-Gal4/UAS-Ptp61f*[HMS00421]. Data are presented as the mean ± SEM of 3 independent experiments. *$p < 0.05$, **$p < 0.005$ (Student's *t*-test).

achieved by using Da-Gal4. Knockdown efficiency of *Ptp61f* RNAi in flies was measured by RT-PCR (Fig. 1F). As shown in Fig. 1D, almost 80% of the rotenone-fed flies died within 48 h, whereas the downregulation of *Ptp61f* significantly suppressed rotenone-induced death. Similarly, approximately 85% of the paraquat-treated flies died within 36 h, however *Ptp61f* knockdown significantly mitigated paraquat toxicity (Fig. 1E). Taken together, these data suggest that downregulation of PTP1B can mitigate ROS-induced toxicity *in vivo*.
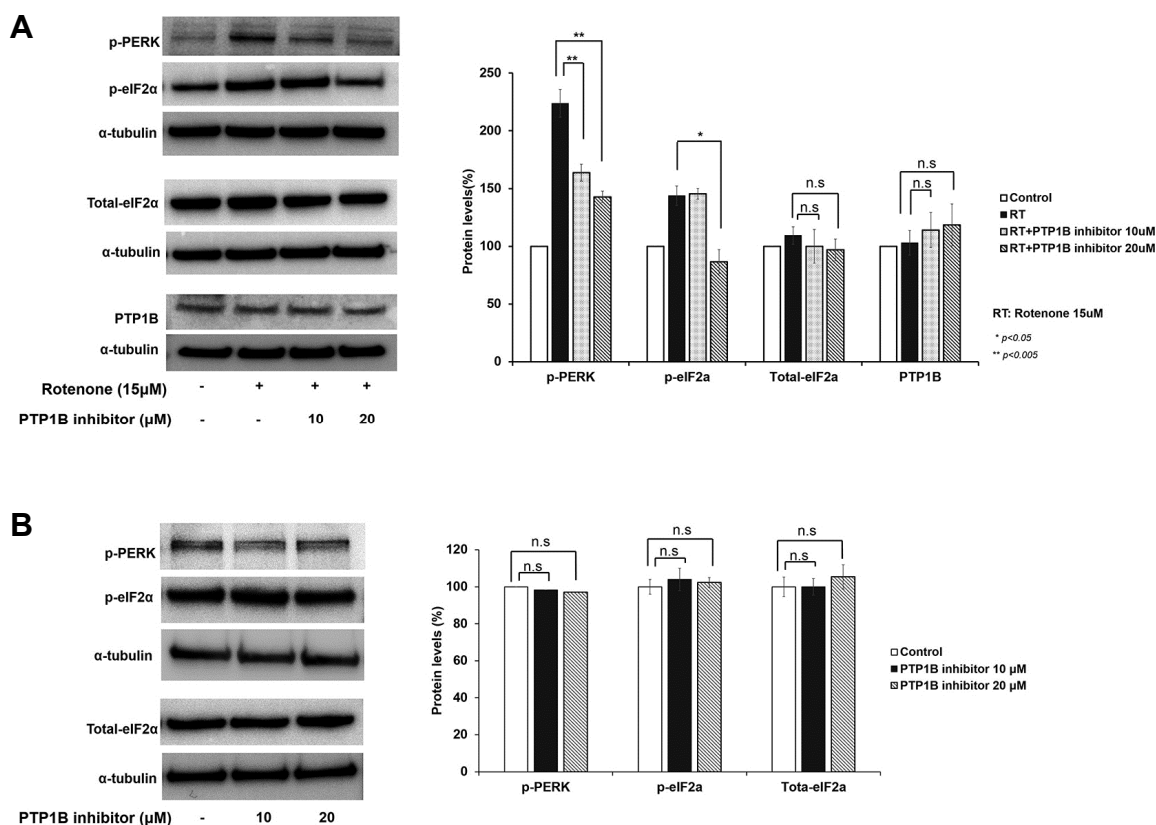
Fig. 2. PTP1B inhibition reduces the level of rotenone-induced ER stress markers. (A) SH-SY5Y cells were pretreated with the PTP1B inhibitor for 30 min and then treated with 15 μM rotenone for 12 h. The expression levels of p-PERK, eIF2α, p-eIF2α and PTP1B were determined with immunoblotting. Rotenone-induced p-PERK and p-eIF2α protein levels were decreased by PTP1B inhibition. (B) SH-SY5Y cells were pretreated with the PTP1B inhibitor for 30 min. The expression levels of p-PERK, eIF2α and p-eIF2α were determined with immunoblotting. There were no significant changes in p-PERK, p-eIF2α and eIF2α with PTP1B inhibitor treatment. The relative protein levels of p-PERK, eIF2α, p-eIF2α and PTP1B imaged by Fusion imaging systems were measured by densitometry and normalized to the expression of α-tubulin. *$p < 0.05$, n.s. (not significant) (One-way ANOVA with Tukey's multiple comparison test).

PTP1B inhibition reduces ER stress-induced activation of the PERK-eIF2α pathway

We then wondered how PTP1B inhibition could suppress ROS-induced toxicity. Previous studies have reported that rotenone-induced ER stress increases the phosphorylation level of PERK (Thr981) and eIF2α (Ser51) (Chen et al., 2008). Phospho-PERK and phospho-eIF2α are well-known markers for ER stress. To investigate the role of the ER stress pathway in rotenone-treated neuronal cells, we performed an immunoblotting analysis with the antibodies against phospho-PERK (Thr981), phospho-eIF2α (Ser51), and total eIF2a and PTP1B from rotenone- and/or PTP1B inhibitor-treated SH-SY5Y cells. Interestingly, PTP1B inhibition significantly reduced the rotenone-induced increase in the phosphorylation of PERK-eIF2α (Fig. 2A). In contrast, the total eIF2a and PTP1B protein levels were not changed in rotenone- and PTP1B inhibitor-treated SH-SY5Y cells (Fig. 2A). We confirmed that the PTP1B inhibitor alone had no effect on the levels of phospho-PERK and phospho-eIF2α (Fig. 2B). These results indicated that neuronal ER stress could be mitigated by PTP1B inhibition.

PTP1B inhibition does not affect the rotenone-induced intracellular ROS level and mitochondrial dysfunction

Previous studies have shown that reduced mitochondrial complex I activity by rotenone treatment results in an increased production of ROS and thereby consequently induces ER stress-mediated neurotoxicity (Goswami et al., 2016). Therefore, rotenone-induced ROS production may be regulated by PTP1B.

To investigate this possibility, we measured intracellular ROS using the redox-sensitive fluorophore 2′,7′-dichlorofluorescein diacetate (DCFH-DA). Non-fluorescent DCFH-DA is converted to the fluorescent molecule DCF by oxidation. We found that the level of DCF in SH-SY5Y cells treated with 15 μM rotenone was significantly increased in a time-dependent manner (Fig. 3A). ROS levels, when stimulated by 15 μM rotenone, peaked at 24 h and were 1.8-fold higher than in the DMSO treatment group. Next, SH-SY5Y cells were pre-incubated with the PTP1B inhibitor (20 μM) for 30
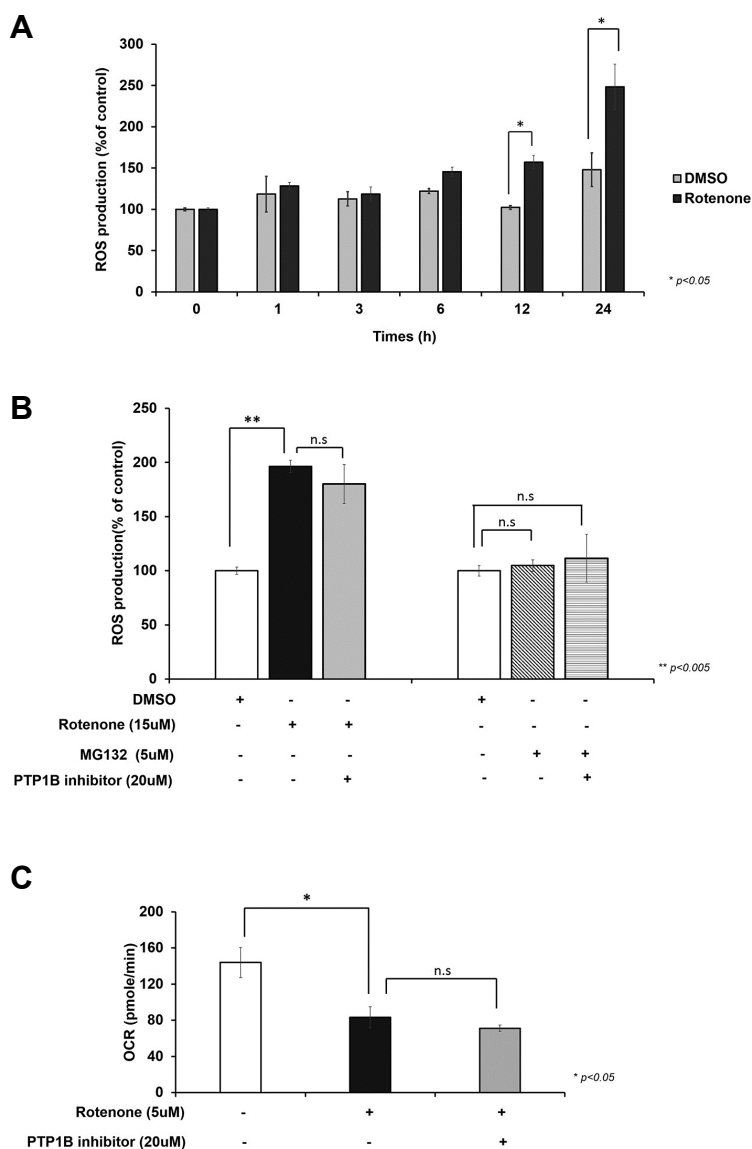
A

B

C

Fig. 3. PTP1B inhibition does not affect intracellular ROS levels. (A) Rotenone induces intracellular ROS production in SH-SY5Y cells. The indicated cells were treated with rotenone (15 μM) for 0-24 h, followed by ROS production using the dye DCFH-DA. The rotenone-induced ROS production was time-dependent. *$p <$ 0.05* when compared with DMSO-treated cells (Student's *t*-test). (B) SH-SY5Y cells were pre-incubated with the PTP1B inhibitor (20 μM) for 30 min and treated with 15 μM rotenone or 5 μM MG132 for 24 h. Intracellular ROS production was detected using the dye DCFH-DA. PTP1B inhibition did not affect rotenone- or MG132-induced ROS production. Moreover, MG132 did not affect the level of ROS production. All data are expressed as the means ± SD (n = 3). **$p <$ 0.005*, n.s (not significant) (One-way ANOVA with Tukey's multiple comparison test). (C) SH-SY5Y cells were pre-treated with the PTP1B inhibitor (20 μM) for 30 min in the indicated medium with or without rotenone (5 μM). The rotenone-treated groups were significantly different from their control groups. The oxygen consumption rate (OCR) was determined using the FX24 instrument for metabolic flux analysis. PTP1B inhibition did not affect the reduction in OCR by rotenone treatment. All data are expressed as the means ± SD (n = 3). *$p <$ 0.05*, n.s. (not significant) (One-way ANOVA with Tukey's multiple comparison test).

min and treated with 15 μM rotenone or 5 μM MG132 for 24 h. Pre-treatment with the PTP1B inhibitor for 30 min showed no significant reduction in the rotenone-induced intracellular ROS level. Treatment with the proteasome inhibitor, MG132, for 24 h showed no significant effect on ROS production compared to that observed in the DMSO treatment group (Fig. 3B).

For real-time analysis of mitochondrial oxidation, SH-SY5Y cells were analyzed using an XF-24 extracellular flux analyzer (Seahorse Bioscience Inc). In sequence, SH-SY5Y cells were treated with rotenone (5 μM) in the presence or absence of the PTP1B inhibitor (20 μM), and cellular oxygen consumption rate (OCR) was measured using the XF24 Seahorse Analyzer. As expected, rotenone significantly inhibited the OCR of SH-SY5Y cells; moreover, PTP1B inhibition did not result in any change in the reduced OCR through injection of

rotenone (Fig. 3C). These data suggest that the neuroprotective effect of PTP1B inhibition does not involve ROS production.

PTP1B inhibition attenuates proteasome inhibitor MG132-induced mammalian neuronal cell death

We have shown that PTP1B inhibition could protect rotenone-induced neurotoxicity without reducing ROS production. Therefore, we hypothesized that PTP1B inhibition may primarily attenuate downstream processes of ROS such as ER stress. MG132 is a specific peptide-aldehyde inhibitor of the ubiquitin proteasome and known as an inducer of ER stress. Because unfolded and misfolded proteins are degraded by the proteasome system (Werner et al., 1996), MG132 treatment results in accumulation of misfolded-proteins in the ER, leading to ER stress (Nakajima et al., 2011).
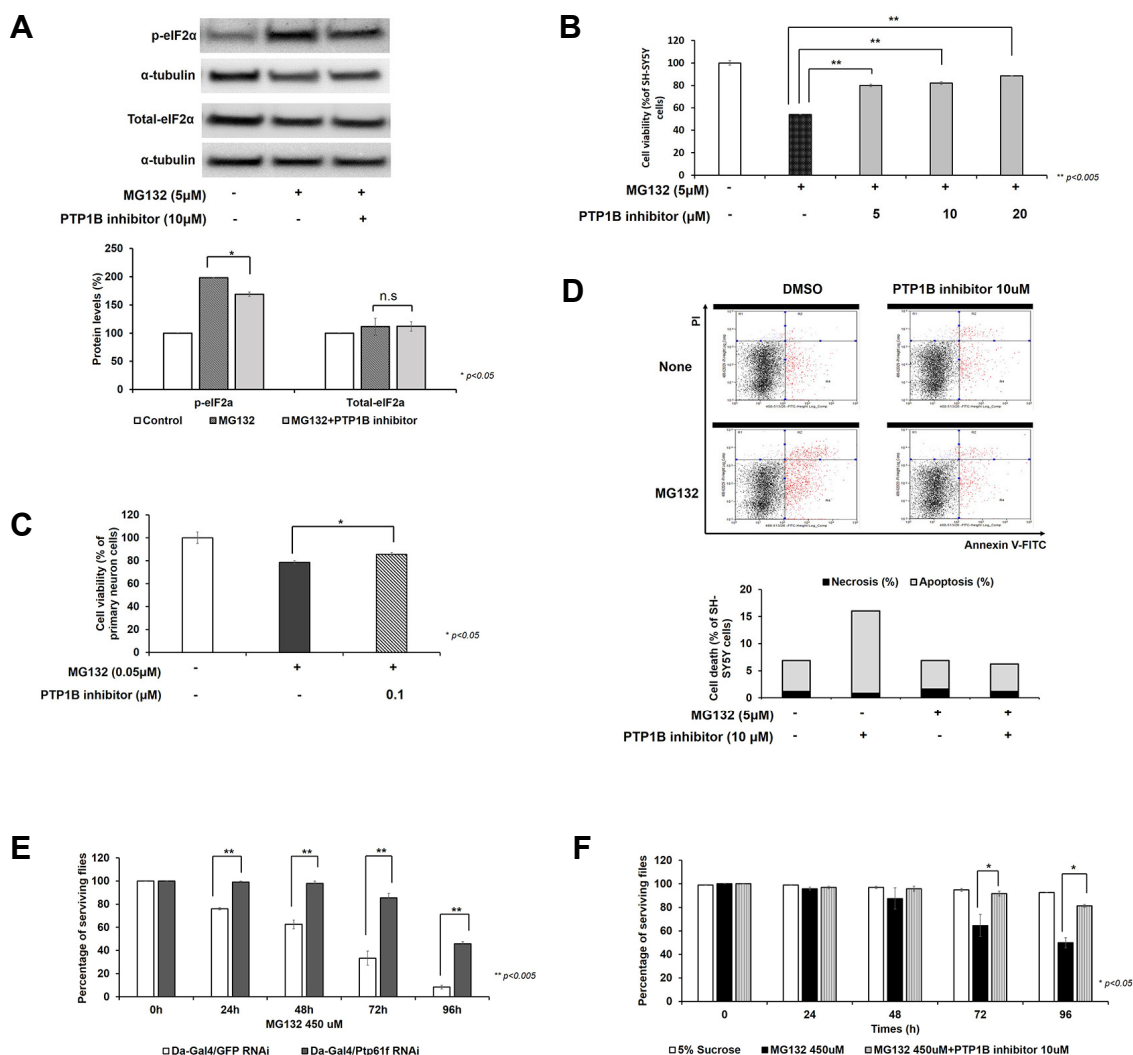
Fig. 4. PTP1B inhibition attenuates proteasome inhibitor, MG132-induced toxicity. (A) SH-SY5Y cells were pretreated with the PTP1B inhibitor for 30 min and then treated with 5 μM MG132 for 24 h. The expression levels of eIF2α and p-eIF2α were determined by immunoblotting. The relative protein levels of eIF2α and p-eIF2α imaged by a Fusion imaging system were measured by densitometry and normalized to the expression of α-tubulin. SH-SY5Y cells (B) and primary mouse cortical neurons (C) were pretreated with various concentrations of the PTP1B inhibitor for 30 min and treated with MG132 for 24 h. The MG132-induced neuronal cell death was attenuated by PTP1B inhibition. Cell viability was then determined by CCK-8 assay, and the percent cell viability was plotted as the mean ± SD of the three different experiments (**$p < 0.005$, One-way ANOVA with Tukey's multiple comparison test). (D) SH-SY5Y cells were pretreated with or without the PTP1B inhibitor (10 μM) for 30 min and were then exposed to MG132 for an additional 24 h. Cell death was evaluated using the Annexin V/PI double staining assay analyzed by flow cytometry. Quantification of the percentage of cell death was based on flow cytometric analysis (lower). (E) *Ptp61f* (*Drosophila* homolog of mammalian PTP1B) RNAi in whole tissue (Da-Gal4) improves survival rates following exposure to 450 μM MG132. Quantification of the percentage of surviving flies. The MG132-reduced lifespan was significantly extended by downregulation of *Ptp61f* in the whole body. There were 96 flies in each group, and the experiment was repeated 3 times in parallel. (F) W^{1118} flies were exposed to 450 μM MG132 in the presence or absence of 10 μM PTP1B inhibitor. There were 60 flies in each group, and experiment was repeated 3 times in parallel. Quantification of the percentage of surviving flies. Data are presented as the mean ± SEM of 3 independent experiments. *$p < 0.05$, **$p < 0.005$ (Student's t-test).

We examined the level of ER stress markers in MG132-treated SH-SY5Y cells. Cells were treated with MG132 for different time periods and subjected to immunoblot analysis. MG132 treatment rapidly increased the level of the ER stress marker, phospho-eIF2α. Moreover, PTP1B inhibition significantly reduced the MG132-induced eIF2α phosphorylation (Fig. 4A). To elucidate the role of PTP1B in neuronal UPS impairment, we treated SH-SY5Y cells (Fig. 4B) and mouse primary cortical neurons (Fig. 4C) with MG132 and/or the PTP1B inhibitor. Cell viability was examined using cell count-

ing kit-8. We found that within the 24-h treatment period, MG132 caused dramatic cell death, while the PTP1B inhibitor suppressed this MG132-induced cell death. To confirm the effect of the PTP1B inhibitor on MG132-induced neuronal cell death, SH-SY5Y cells were double-labeled for Annexin V and PI and then analyzed by flow cytometric analysis. MG132 induced cell death in 16.03% of SH-SY5Y cells (PI⁻/Annexin V⁺ or PI⁺/Annexin V⁺: 15.22% and PI⁺/Annexin V⁻: 0.81%). In comparison, the percent cell death in SH-SY5Y cells treated with both MG132 and the PTP1B inhibitor was 6.22% (PI⁻/Annexin V⁺ or PI⁺/Annexin V⁺: 5.03% and PI⁺/Annexin V⁻: 1.19%) (Fig. 4D).

PTP1B inhibition mitigates MG132-induced toxicity in Drosophila

To test the idea that therapeutic modulation of PTP1B may have an effect on toxicity induced by UPS impairment *in vivo*, we turned back to the fly. We next tested the role of PTP1B in MG132-induced toxicity *in vivo* using *Drosophila*. We

knocked down *Ptp61f* by RNAi in the presence of MG132 and examined the effect of PTP1B knockdown on the MG132-induced death of flies. As shown in Fig. 4E, almost 90% of the MG132-fed flies died within 96 h, whereas the downregulation of *Ptp61f* significantly suppressed MG132-induced death. Furthermore, we tested whether treating flies with the PTP1B inhibitor (CAS 765317-72-4) could affect MG132-induced toxicity. Flies fed 10 μM PTP1B inhibitor showed markedly mitigated MG132-induced toxicity. As shown in Fig. 4F, feeding flies with MG132 and 10 μM PTP1B inhibitor increased the survival rate compared to flies that were fed MG132 without the PTP1B inhibitor. Taken together, these data suggest that downregulation of PTP1B can mitigate proteasome inhibitor, MG132-induced toxicity *in vivo*.

PTP1B inhibition protects against neuronal cell death by the another ER stress inducer, tunicamycin

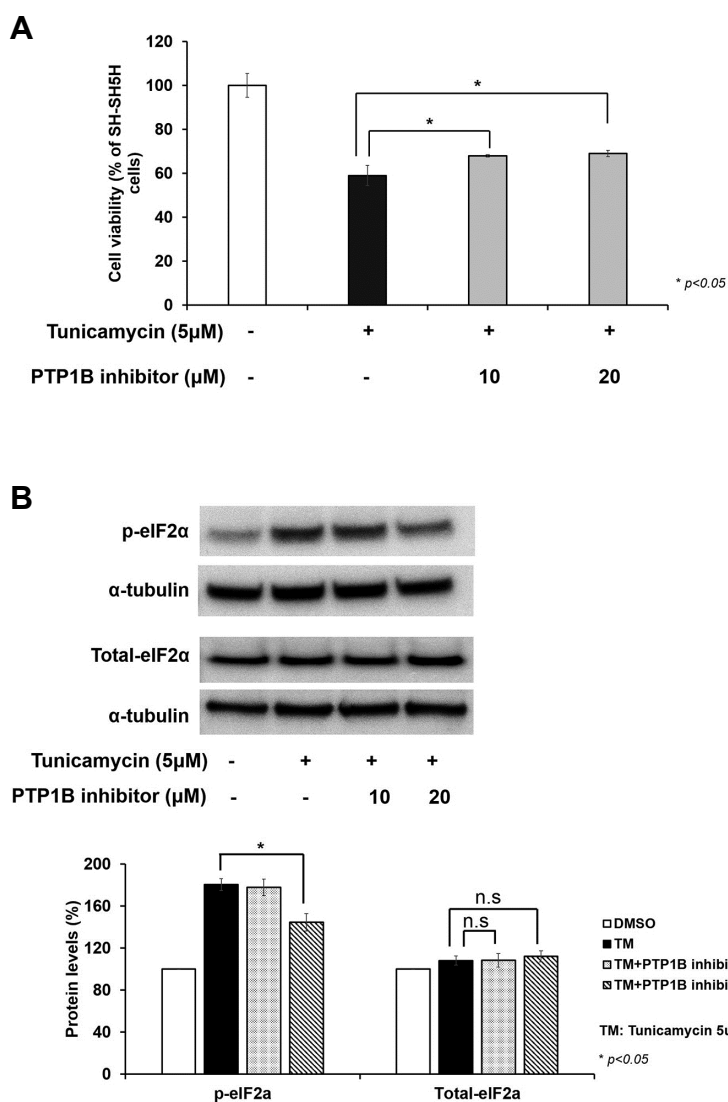Tunicamycin specifically blocks the initial step of glycoprotein

A

B

Fig. 5. ER stress inducer, tunicamycin-induced toxicity is mitigated by PTP1B inhibition. (A) SH-SY5Y cells were pretreated with various concentrations of the PTP1B inhibitor for 30 min and then treated with 5 μM tunicamycin for 24 h. The tunicamycin-induced increase in neuronal cell death was attenuated by PTP1B inhibition. The cell viability was then determined by CCK-8 assay, and the percentage of cell viability was plotted as the mean ± SD of the three different experiments ($*p < 0.05$, One-way ANOVA with Tukey's multiple comparison test). (B) SH-SY5Y cells were pretreated with the PTP1B inhibitor for 30 min and then treated with 5 μM tunicamycin for 6 h. Tunicamycin-induced p-eIF2α protein level was decreased by PTP1B inhibition. The relative protein levels of eIF2α and p-eIF2α imaged by Fusion imaging systems were measured by densitometry and normalized to the expression of α-tubulin. $*p < 0.05$, n.s. (not significant) (One-way ANOVA with Tukey's multiple comparison test).

biosynthesis in the ER (Oslowski and Urano, 2011). Moreover, a previous study showed that tunicamycin is induced in neuronal cell death and ER stress. Thus, we sought to confirm how the neuroprotective effect of PTP1B is regulated by other ER stress inducers in SH-SY5Y cells.

SH-SY5Y cells were treated with 5 μM of tunicamycin for 24 h and pre-treated with different dosages of the PTP1B inhibitor for 30 min. The cell viability was tested using the CCK-8 assay. The result of the CCK-8 assay indicated that PTP1B inhibition (20 μM) prevented cell death induced by tunicamycin (Fig. 5A, 30.8% compared to 40.9% in tunicamycin-treated SH-SY5Y cells). These data indicate that PTP1B plays an important role in various forms of ER stress-induced neuronal toxicity. Next, we also examined whether PTP1B inhibition influences tunicamycin-induced ER stress. PTP1B inhibition significantly reduced the tunicamycin-induced increase in the phosphorylation of eIF2α (Fig. 5B). These results suggest that PTP1B inhibition attenuates the toxicity of neuronal ER stress.

DISCUSSION

Oxidative stress and UPS impairment are common features of many neurodegenerative diseases including AD, PD and ALS. Both cause accumulation of misfolded and unfolded proteins in the ER lumen, and accumulation of these abnormal proteins induces ER stress. ER stress activates a stress-adaptive signaling process called the unfolded protein response (UPR) (Xiang et al., 2017). UPR activation is mediated via three ER stress sensors localized in the ER lumen: IRE1, ATF6 and PERK. Recently, many studies have reported that phosphorylated PERK and eIF2α are detected in postmortem brain and spinal cord tissue from AD, ALS, PD and frontotemporal dementia (FTD) patients (Smith and Mallucci, 2016). Moreover, pharmacological inhibition of the PERK pathway restored pathological features of ALS, Prion disease and FTD animal models (Kim et al., 2014; Moreno et al., 2013; Radford et al., 2015). Therefore, the PERK-eIF2α axis of the UPR might be a valuable therapeutic target for various neurodegenerative diseases.

PTP1B is a negative regulator of insulin signaling and is predominantly localized to the cytoplasmic surface of the ER (Popov, 2012). Recent studies have suggested that PTP1B is implicated in the regulation of ER stress signaling in cultured adipocytes and myotubes (Bettaieb et al., 2012; Panzhinskiy et al., 2013b). Interestingly, Song et al. (2016) discovered that inhibition of PTP1B has an anti-inflammatory effect in a mouse neuroinflammation model. Many reports have indicated that inflammatory responses are also implicated in ER stress and chronic metabolic diseases such as type 2 diabetes, obesity and insulin resistance (Hotamisligil, 2010; Zhang, 2010). Furthermore, Hakim et al. (2015) showed that chronic sleep fragmentation induces ER stress and PTP1B upregulation in hypothalamic neurons. Collectively, previous studies have suggested that PTP1B might modulate the toxic effect of neuronal ER stress.

To elucidate the relationship between neuronal ER stress and PTP1B, we examined whether neuronal toxicity induced by UPS impairment and ROS production were mitigated by PTP1B inhibition.

We showed that PTP1B inhibition attenuated oxidative stress- and UPS impairment-induced toxicity in *Drosophila* and mammalian neuronal cells. Furthermore, PTP1B inhibition decreased the level of ER stress markers such as eIF2 alpha phosphorylation (Ser51) and PERK phosphorylation (Thr981) under oxidative stress. Both serine/threonine and tyrosine phosphorylation of PERK are essential for optimal kinase activity of PERK (Su et al., 2008). Moreover, PTP1B dephosphorylates the tyrosine phosphorylation site of PERK in adipocytes (Bettaieb et al., 2012). IRE1 signaling, another UPR pathway, is also potentiated by PTP1B during ER stress in mouse embryonic fibroblasts (Gu et al., 2004). However, we found that PTP1B inhibition does not affect phosphorylation level of eIF2 alpha and PERK in non-stressed neuronal cells. Therefore, neuroprotective effect of PTP1B inhibition is not due to direct modulation of the UPR pathway by PTP1B.

To the best of our knowledge, rotenone triggers massive ROS production through the inhibition of mitochondrial complex I, which finally results in ER stress and apoptotic cell death (Seoposengwe et al., 2013; Swarnkar et al., 2012). Therefore, PTP1B inhibition might mitigate rotenone-induced ROS production via improvement of mitochondrial function. Our study showed that significantly increased levels of ROS and mitochondria dysfunction were observed in rotenone-treated neuronal cells. However, the increase in ROS production and mitochondrial dysfunction induced by rotenone treatment were not altered by PTP1B inhibition. These data demonstrate that the protective effect of PTP1B inhibition seems to not be related to ROS production or mitochondrial activity.

We also tested the effect of the PTP1B inhibitor after inducing ER stress with tunicamycin. Tunicamycin inhibits the glycosylation of newly synthesized protein, and this biosynthetic step occurs within the ER. Consequently, impairment of protein glycosylation leads to the disruption of proper protein folding in the ER (Foufelle and Fromenty, 2016). We found that tunicamycin-induced cell death and eIF2α phosphorylation is also suppressed by PTP1B inhibition in SH-SY5Y cells. Taken together, these results suggest that PTP1B inhibition attenuates the toxicity of neuronal ER stress.

Possible neuroprotective mechanisms of PTP1B inhibition include BDNF/TrkB signaling. TrkB is a family of receptor tyrosine-kinases (RTKs) and a receptor of brain-derived neurotrophic factor (Vieira et al., 2017). Many studies have reported that the toxic effects of ER stress are significantly mitigated by the upregulation of BDNF in the brain and neuronal cells (Chen et al., 2007; Qiu et al., 2013; Shimoke et al., 2004; Wei et al., 2014; Zhu et al., 2004). Moreover, TrkB is a direct substrate of PTP1B; so, PTP1B negatively regulates TrkB activation via BDNF treatment (Ozek et al., 2014). Notably, deletion or inhibition of PTP1B potentiates BDNF signaling via enhanced TrkB phosphorylation in SH-SY5Y cells and the mouse hypothalamic brain region (Ozek et al., 2014). Therefore, PTP1B inhibition might mitigate the toxic consequences of neuronal ER stress via enhancing BDNF/TrkB signaling.

Another possible mechanism is the nuclear factor (erythroid-derived 2)-like 2 (Nrf2) pathway. Nrf2 is a basic

leucine-zipper transcription factor that plays an important role in mitigating proteotoxic stress (Pajares et al., 2017). Under normal conditions, the level of Nrf2 protein remains low because of its rapid turnover. In response to different stimuli, including accumulation of misfolded proteins, the Nrf2 protein is increased and translocated to the nucleus to promote the transcription of ARE-containing genes (Cui et al., 2016). Nrf2 activation upregulates key genes for the protein quality control system, and this gene upregulation promotes the degradation of misfolded proteins. Specifically, Nrf2 increases the expression level of several UPS subunits and protects cells from abnormal protein accumulation. Previous studies have indicated that Nrf2 activation is essential for transcriptional upregulation of the 26S proteasome subunit and improving proteasome activity in the liver and fibroblasts (Kapeta et al., 2010; Kwak et al., 2003a; 2003b; Pickering et al., 2012). Moreover, PTP1B deficiency enhances the nuclear accumulation of Nrf2 in acetaminophen-induced hepatotoxicity via the GSK3 beta/Src-Fyn pathway (Mobasher et al., 2013). In this study, we found that UPS impairment-induced toxicity is rescued by PTP1B inhibition. Therefore, PTP1B inhibition might mitigate neuronal ER stress by promoting the degradation of abnormal proteins through Nrf2 activation.

In conclusion, our study showed that PTP1B inhibition attenuates ER stress via mitochondria-independent mechanisms in neuronal cells. As a proof of principle that modulating PTP1B activity could be beneficial, a small molecule inhibitor of PTP1B significantly suppressed UPS impairment-induced toxicity *in vivo* in *Drosophila*. Thus, molecules that decrease PTP1B activity could represent a promising avenue for the treatment of neurodegenerative diseases implicated in ER stress. However, further studies are needed to elucidate the detailed molecular mechanism underlying neuroprotection via PTP1B inhibition.

ACKNOWLEDGMENTS

REFERENCES

Araki, W., Yuasa, K., Takeda, S., Shirotani, K., Takahashi, K., and Tabira, T. (2000). Overexpression of presenilin-2 enhances apoptotic death of cultured cortical neurons. Ann. N. Y. Acad. Sci. *920*, 241-244.

Bettaieb, A., Matsuo, K., Matsuo, I., Wang, S., Melhem, R., Koromilas, A.E., and Haj, F.G. (2012). Protein tyrosine phosphatase 1B deficiency potentiates PERK/eIF2α signaling in brown adipocytes. PLoS One *7*, e32212.

Chen, G., Fan, Z., Wang, X., Ma, C., Bower, K.A., Shi, X., Ke, Z.J., and Luo, J. (2007). Brain-derived neurotrophic factor suppresses tunicamycin-induced upregulation of CHOP in neurons. J. Neurosci. Res. *85*, 1674-1684.

Chen, Y.Y., Chen, G., Fan, Z., Luo, J., and Ke, Z.J. (2008). GSK3beta and endoplasmic reticulum stress mediate rotenone-induced death of SK-N-MC neuroblastoma cells. Biochem. Pharmacol. *76*, 128-138.

Chung, J., Kim, K.H., Lee, S.C., An, S.H., and Kwon, K. (2015). Ursodeoxycholic acid (UDCA) exerts anti-atherogenic effects by inhibiting endoplasmic reticulum (ER) stress induced by disturbed flow. Mol. Cells *38*, 851-858.

Cui, W., Bai, Y., Luo, P., Miao, L., and Cai, L. (2013). Preventive and therapeutic effects of MG132 by activating Nrf2-ARE signaling pathway on oxidative stress-induced cardiovascular and renal injury. Oxid. Med. Cell. Longev. *2013*, 306073.

Cui, T., Lai, Y., Janicki, J.S., and Wang, X. (2016). Nuclear factor erythroid-2 related factor 2 (Nrf2)-mediated protein quality control in cardiomyocytes. Front. Biosci. (Landmark Ed.) *21*, 192-202.

Day, B.J., Patel, M., Calavetta, L., Chang, L.Y., and Stamler, J.S. (1999). A mechanism of paraquat toxicity involving nitric oxide synthase. Proc. Natl. Acad. Sci. USA *96*, 12760-12765.

Foufelle, F., and Fromenty, B. (2016). Role of endoplasmic reticulum stress in drug-induced toxicity. Pharmacol. Res. Perspect. *4*, e00211.

Goswami, P., Gupta, S., Biswas, J., Joshi, N., Swarnkar, S., Nath, C., and Singh, S. (2016). Endoplasmic reticulum stress plays a key role in rotenone-induced apoptotic death of neurons. Mol. Neurobiol. *53*, 285-298.

Gu, F., Nguyên, D.T., Stuible, M., Dubé, N., Tremblay, M.L., and Chevet, E. (2004). Protein-tyrosine phosphatase 1B potentiates IRE1 signaling during endoplasmic reticulum stress. J. Biol. Chem. *279*, 49689-49693.

Hakim, F., Wang, Y., Carreras, A., Hirotsu, C., Zhang, J., Peris, E., and Gozal, D. (2015). Chronic sleep fragmentation during the sleep period induces hypothalamic endoplasmic reticulum stress and PTP1b-mediated leptin resistance in male mice. Sleep *38*, 31-40.

Hardie, R.A., van Dam, E., Cowley, M., Han, T.L., Balaban, S., Pajic, M., Pinese, M., Iconomou, M., Shearer, R.F., McKenna, J., et al. (2017). Mitochondrial mutations and metabolic adaptation in pancreatic cancer. Cancer Metab. *5*, 2.

Hotamisligil, G.S. (2010). Endoplasmic reticulum stress and the inflammatory basis of metabolic disease. Cell *140*, 900-917.

Kapeta, S., Chondrogianni, N., and Gonos, E.S. (2010). Nuclear erythroid factor 2-mediated proteasome activation delays senescence in human fibroblasts. J. Biol. Chem. *285*, 8171-8184.

Kim, H.J., Raphael, A.R., LaDow, E.S., McGurk, L., Weber, R.A., Trojanowski, J.Q., Lee, V.M., Finkbeiner, S., Gitler, A.D., and Bonini, N.M. (2014). Therapeutic modulation of eIF2α phosphorylation rescues TDP-43 toxicity in amyotrophic lateral sclerosis disease models. Nat. Genet. *46*, 152-160.

Kwak, M.K., Wakabayashi, N., Greenlaw, J.L., Yamamoto, M., and Kensler, T.W. (2003a). Antioxidants enhance mammalian proteasome expression through the Keap1-Nrf2 signaling pathway. Mol. Cell. Biol. *23*, 8786-8794.

Kwak, M.K., Wakabayashi, N., Itoh, K., Motohashi, H., Yamamoto, M., and Kensler, T.W. (2003b). Modulation of gene expression by cancer chemopreventive dithiolethiones through the Keap1-Nrf2 pathway. Identification of novel gene clusters for cell survival. J. Biol. Chem. *278*, 8135-8145.

Mobasher, M.A., Gonzalez-Rodriguez, A., Santamaria, B., Ramos, S., Martin, M.A., Goya, L., and Valverde, A.M. (2013). Protein tyrosine phosphatase 1B modulates GSK3beta/Nrf2 and IGFIR signaling pathways in acetaminophen-induced hepatotoxicity. Cell Death Dis. *4*, e626.

Moreno, J.A., Halliday, M., Molloy, C., Radford, H., Verity, N., Axten, J.M., Ortori, C.A., Willis, A.E., Fischer, P.M., Barrett, D.A., et al. (2013). Oral treatment targeting the unfolded protein response prevents neurodegeneration and clinical disease in prion-infected mice. Sci. Transl. Med. *5*, 206ra138.

Nakajima, S., Kato, H., Takahashi, S., Johno, H., and Kitamura, M. (2011). Inhibition of NF-kappaB by MG132 through ER stress-mediated induction of LAP and LIP. FEBS Lett. *585*, 2249-2254.

Nandipati, S., and Litvan, I. (2016). Environmental Exposures and Parkinson's Disease. Int. J. Environ. Res. Public Health *13*, 881.

Oslowski, C.M., and Urano, F. (2011). Measuring ER stress and the unfolded protein response using mammalian tissue culture system. Methods Enzymol. *490*, 71-92.

Ozcan, L., and Tabas, I. (2012). Role of endoplasmic reticulum stress in metabolic disease and other disorders. Annu. Rev. Med. *63*, 317-328.

Ozek, C., Kanoski, S.E., Zhang, Z.Y., Grill, H.J., and Bence, K.K. (2014). Protein-tyrosine phosphatase 1B (PTP1B) is a novel regulator of central brain-derived neurotrophic factor and tropomyosin receptor kinase B (TrkB) signaling. J. Biol. Chem. *289*, 31682-31692.

Pajares, M., Cuadrado, A., and Rojo, A.I. (2017). Modulation of proteostasis by transcription factor NRF2 and impact in neurodegenerative diseases. Redox Biol. *11*, 543-553.

Pal, R., Monroe, T.O., Palmieri, M., Sardiello, M., and Rodney, G.G. (2014). Rotenone induces neurotoxicity through Rac1-dependent activation of NADPH oxidase in SHSY-5Y cells. FEBS Lett. *588*, 472-481.

Panzhinskiy, E., Ren, J., and Nair, S. (2013a). Protein tyrosine phosphatase 1B and insulin resistance: role of endoplasmic reticulum stress/reactive oxygen species/nuclear factor kappa B axis. PLoS One *8*, e77228.

Panzhinskiy, E., Hua, Y., Culver, B., Ren, J., and Nair, S. (2013b). Endoplasmic reticulum stress upregulates protein tyrosine phosphatase 1B and impairs glucose uptake in cultured myotubes. Diabetologia *56*, 598-607.

Pickering, A.M., Linder, R.A., Zhang, H., Forman, H.J., and Davies, K.J. (2012). Nrf2-dependent induction of proteasome and Pa28αβ regulator are required for adaptation to oxidative stress. J. Biol. Chem. *287*, 10021-10031.

Popov, D. (2012). Endoplasmic reticulum stress and the on site function of resident PTP1B. Biochem. Biophys. Res. Commun. *422*, 535-538.

Prada, P.O., Quaresma, P.G., Caricilli, A.M., Santos, A.C., Guadagnini, D., Morari, J., Weissmann, L., Ropelle, E.R., Carvalheira, J.B., Velloso, L.A., et al. (2013). Tub has a key role in insulin and leptin signaling and action in vivo in hypothalamic nuclei. Diabetes *62*, 137-148.

Qiu, B., Hu, S., Liu, L., Chen, M., Wang, L., Zeng, X., and Zhu, S. (2013). CART attenuates endoplasmic reticulum stress response induced by cerebral ischemia and reperfusion through upregulating BDNF synthesis and secretion. Biochem. Biophys. Res. Commun. *436*, 655-659.

Radford, H., Moreno, J.A., Verity, N., Halliday, M., and Mallucci, G.R. (2015). PERK inhibition prevents tau-mediated neurodegeneration in a mouse model of frontotemporal dementia. Acta Neuropathol. *130*, 633-642.

Seoposengwe, K., van Tonder, J.J., and Steenkamp, V. (2013). *In vitro* neuroprotective potential of four medicinal plants against rotenone-induced toxicity in SH-SY5Y neuroblastoma cells. BMC Complement. Altern. Med. *13*, 353.

Shimoke, K., Utsumi, T., Kishi, S., Nishimura, M., Sasaya, H., Kudo, M., and Ikeuchi, T. (2004). Prevention of endoplasmic reticulum stress-induced cell death by brain-derived neurotrophic factor in cultured cerebral cortical neurons. Brain Res. *1028*, 105-111.

Smith, H.L., and Mallucci, G.R. (2016). The unfolded protein response: mechanisms and therapy of neurodegeneration. Brain *139*, 2113-2121.

Song, J.X., Choi, M.Y., Wong, K.C., Chung, W.W., Sze, S.C., Ng, T.B., and Zhang, K.Y. (2012) Baicalein antagonizes rotenone-induced apoptosis in dopaminergic SH-SY5Y cells related to Parkinsonism. Chin. Med. *7*, 1.

Song, G.J., Jung, M., Kim, J.H., Park, H., Rahman, M.H., Zhang, S., Zhang, Z.Y., Park, D.H., Kook, H., Lee, I.K., et al. (2016). A novel role for protein tyrosine phosphatase 1B as a positive regulator of neuroinflammation. J. Neuroinflammation *13*, 86.

Su, Q., Wang, S., Gao, H.Q., Kazemi, S., Harding, H.P., Ron, D., and Koromilas, A.E. (2008). Modulation of the eukaryotic initiation factor 2 alpha-subunit kinase PERK by tyrosine phosphorylation. J. Biol. Chem. *283*, 469-475.

Swarnkar, S., Goswami, P., Kamat, P.K., Gupta, S., Patro, I.K., Singh, S., and Nath, C. (2012). Rotenone-induced apoptosis and role of calcium: a study on Neuro-2a cells. Arch. Toxicol. *86*, 1387-1397.

Vieira, M.N., Lyra E Silva, N.M., Ferreira, S.T., and De Felice, F.G. (2017). Protein tyrosine phosphatase 1B (PTP1B): a potential target for Alzheimer's therapy? Front. Aging Neurosci. *9*, 7.

Werner, E.D., Brodsky, J.L., and McCracken, A.A. (1996). Proteasome-dependent endoplasmic reticulum-associated protein degradation: an unconventional route to a familiar fate. Proc. Natl. Acad. Sci. USA *93*, 13797-13801.

Wei, H.J., Xu, J.H., Li, M.H., Tang, J.P., Zou, W., Zhang, P., Wang, L., Wang, C.Y., and Tang, X.Q. (2014). Hydrogen sulfide inhibits homocysteine-induced endoplasmic reticulum stress and neuronal apoptosis in rat hippocampus via upregulation of the BDNF-TrkB pathway. Acta Pharmacol. Sin. *35*, 707-715.

Wiesmann, C., Barr, K.J., Kung, J., Zhu, J., Erlanson, D.A., Shen, W., Fahr, B.J., Zhong, M., Taylor, L., Randal, M., et al. (2004). Allosteric inhibition of protein tyrosine phosphatase 1B. Nat. Struct. Mol. Biol. *11*, 730-737.

Xiang, C., Wang, Y., Zhang, H., and Han, F. (2017). The role of endoplasmic reticulum stress in neurodegenerative disease. Apoptosis *22*, 1-26.

Xu, C., Bailly-Maitre, B., and Reed, J.C. (2005). Endoplasmic reticulum stress: cell life and death decisions. J. Clin. Invest. *115*, 2656-2664.

Xu, Y., Liu, X., Guo, F., Ning, Y., Zhi, X., Wang, X., Chen, S., Yin, L., and Li, X. (2012). Effect of estrogen sulfation by SULT1E1 and PAPSS on the development of estrogen-dependent cancers. Cancer Sci. *103*, 1000-1009.

Zhang, K. (2010). Integration of ER stress, oxidative stress and the inflammatory response in health and disease. Int. J. Clin. Exp. Med. *3*, 33-40.

Zhu, W., Bijur, G.N., Styles, N.A., and Li, X. (2004). Regulation of FOXO3a by brain-derived neurotrophic factor in differentiated human SH-SY5Y neuroblastoma cells. Brain Res. Mol. Brain Res. *126*, 45-56.

Zhu, X., Zhou, Y., Tao, R., Zhao, J., Chen, J., Liu, C., Xu, Z., Bao, G., Zhang, J., Chen, M., et al. (2015). Upregulation of PTP1B after rat spinal cord injury. Inflammation *38*, 1891-1902.